# High-Fidelity Time-Stepping for Reverse-Time Migration

Ben Wards*
University of Calgary, Calgary, AB
bdwards@ucalgary.ca

and

Gary Margrave and Michael Lamoureux
University of Calgary, Calgary, AB, Canada

## Summary

As a result of the numerical performance of finite-difference operators, reverse-time migration (RTM) images are typically low frequency. We consider an alternative to wavefield propagation with finite differences, a high-fidelity time-stepping equation based on the Fourier transform, which is exact for homogeneous media if an aliasing condition is met. The technique is adapted to variable velocity using a localized Fourier transform (Gabor transform). The feasibility of using the time-stepping equation for RTM is demonstrated by studying its stability properties, its impulse response, and by migrating a synthetic example of a salt dome. We show that a high frequency wavefield can be time stepped with no loss of frequency content and with a much larger time step than is commonly used.

## Introduction

Reverse-time migration (Baysal, 1983; McMechan, 1983) is a very powerful depth migration algorithm. It is capable of imaging reflectors using overturned waves and multiples. However, as a result of the sampling requirements, processing seismic surveys will either require harsh filtering to remove higher frequency data or they will require long run times even with a cluster of computers. The fine sampling requirements occur because finite-difference operators propagate high frequencies with an incorrect dispersion relation. An example of the impressive performance, yet low frequency response, is the method is Jones et al. (2007).

We propose an alternative time-stepping equation that does not use finite differences. Our equation can time-step a wavefield using a coarser time step because the spatial derivatives in the wave equation are computed exactly in the Fourier domain and so do not suffer from dispersion at high frequencies. As a result, the sampling requirements are better than propagating with finite differences. The fundamental limitation on the time-step size in our method arises from a temporal aliasing condition, which we derive. The accuracy and stability properties are demonstrated by comparing solutions of the time-stepping equation to finite-difference solutions. We extend our method to variable velocity by replacing the global Fourier transform with a local Gabor transform using localizing windows within which a locally homogeneous solution is computed.

## Theory

The Fourier transform over the spatial dimensions converts the constant-velocity scalar wave equation to

$$\left(k_x^2 + k_z^2\right)\hat{U} = \frac{1}{c^2}\hat{U}_{tt}, \tag{1}$$

where $\hat{U}$ is the amplitude of the wavefield in the Fourier domain, $\hat{U}_{tt}$ is the second time derivative of the wavefield, $x$ is the lateral coordinate, $z$ is the depth coordinate, $t$ is the time coordinate, $c$ is the speed of propagation, $k_x, k_z$ are the wavenumbers which correspond to the coordinates $x, z$, respectively. This equation, for the initial conditions $U(0,x,z)$ and $U_t(0,x,z)$, has the solution

$$\hat{U}\left(\Delta t, k_x, k_z\right) = A\left(k_x, k_z\right)\exp\left(-i\omega\left(k_x, k_z\right)\Delta t\right) + B(k_x, k_z)\exp\left(i\omega\left(k_x, k_z\right)\Delta t\right), \tag{2}$$

where $\omega\left(k_x, k_z\right) = c\sqrt{k_x^{\,2} + k_z^{\,2}}$ and $A\left(k_x, k_z\right)$, $B\left(k_x, k_z\right)$ are determined by the 2D spatial Fourier transforms of $U(0,x,z)$, $U_t(0,x,z)$. However, knowledge of the time derivative of the field at each step is inconvenient so we determine from the field in the present, $U(0,x,z)$ and the field in the past $U\left(-\Delta t, x, z\right)$. This may be done by writing an equation similar to equation (2) for the wavefield $\hat{U}\left(-\Delta t, k_x, k_z\right)$ in terms of $U\left(0,x,z\right)$ and $U_t\left(0,x,z\right)$. Thus we may estimate the wavefield at time $t = \Delta t$ without the knowledge of the first derivative, $U_t\left(0,x,z\right)$. The resulting exact solution of the constant-velocity wave equation is

$$U(\Delta t, x, z) = -U(-\Delta t, x, z) + \frac{1}{\pi^2}\int \hat{U}\left(0, k_x, k_z\right)\cos\left(\omega\left(k_x, k_z\right)\Delta t\right)e^{i\underline{x}\bullet\underline{k}}dk_x dk_z \tag{3}$$

where $\underline{x}\bullet\underline{k}$ is the scalar product of the 2D position and wavenumber vectors. It is a simple exercise to show that for small $\omega\left(k_x, k_z\right)\left|\Delta t\right|$ the cosine in equation (3) can be replaced by its small angle approximation and eventually the usual finite-difference time stepping equation is obtained. While our result is exact for constant velocity, with sampled data the size of the time step is limited by aliasing considerations. When implemented numerically with the fast Fourier transform, equation (3) takes the wavefield at two distinct times with spatial sampling rate $\Delta x$ and generates a new wavefield at a future time. The wavenumber which corresponds to the greatest frequency occurs when $\underline{k} = \left(\pi/\Delta x, \pi/\Delta x\right)$, the Nyquist wavenumbers. By the dispersion relation, the maximum wavenumber generates a frequency $\omega = c\pi\sqrt{2}/\Delta x$. Since the wavefield is sampled in time at rate $\Delta t$, the requirement that temporal frequencies not be aliased means that the Courant number $r$ must satisfy the inequality $r = \Delta t c/\Delta x < 1/\sqrt{2} \sim 0.707$. Figure 1 (c)-(e) demonstrates the instability that results from this aliasing condition on the Courant number. While it is probably more correct to call this effect aliasing, we here use the more standard term "instability". This limitation on the step size is far less restrictive than that usually encountered in finite-difference time stepping.

Figure 1 (a) is the impulse response to a minimum phase wavelet using the second-order finite-difference solution which contains unacceptable high-frequency noise arising from the dispersive propagation of the higher frequencies of the impulse. In contrast, despite a much larger time step, Figure 1 (b) uses equation (3) recursively to calculate the impulse response without high frequency noise.

In RTM it is necessary to propagate a wavefield in a variable velocity medium. To demonstrate how equation (3) can be adapted to a variable velocity model, we consider a $v(z)$ medium where the velocity only varies in the vertical direction. A similar construction where the windowing functions depends, additionally, on the $x$ or lateral coordinate can be used for a general velocity model which has done in a similar context in Ma and Margrave (2007). Using a smooth POU essentially smoothes the velocity model and therefore cannot account for multiple reflections. It is possible to account for reflections by considering windows with discontinuous boundaries.

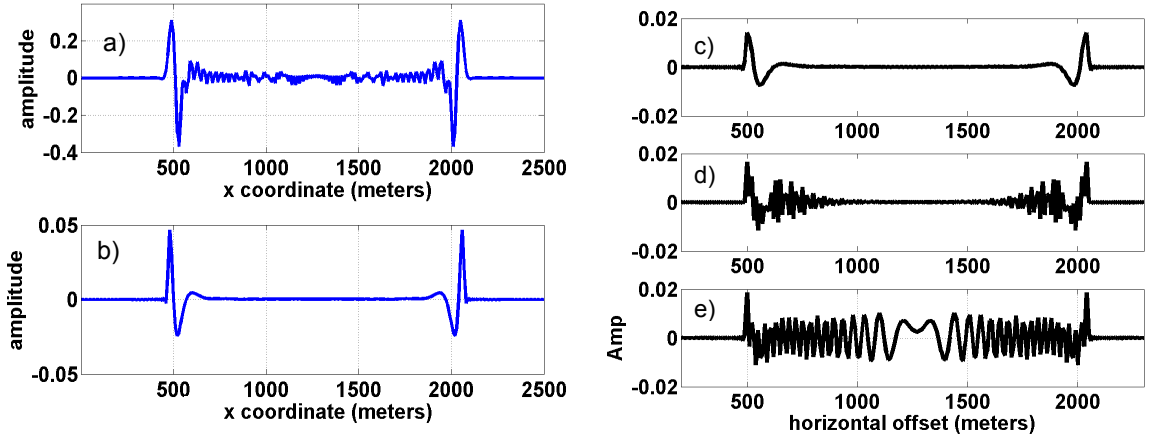


Figure 1: Cross Section through center of the circular wavefront of a propagating minimum phase wavelet. (a) Using 2nd order finite differences with $\Delta t = 0.0001 s$ . (b) Using equation (3) with $\Delta t = 0.001 s$ . The finite-difference time-stepper took 10 times as long to execute. (c)-(e) Comparison of stability of the Courant number $r = 0.6, 0.8,$ and $1.0$ , instability is observed for the two larger Courant numbers.

Consider the partition of unity (POU) $\left\{ \Omega_n(z) = \exp\left( -\frac{(z-an)^2}{2\sigma^2} \right) \Big/ \sum_{m=1}^{N} \exp\left( -\frac{(z-am)^2}{2\sigma^2} \right), n = 1, \ldots, N \right\}$

where $\sum_{n=1}^{N} \Omega_n(z) = 1$ and $0 \le \Omega_n(z) \le 1$ for $0 \le z \le z_{\max}$ and each window $\Omega_n$ is localized at the line $z = an$. The constants $a, \sigma, N$ are chosen so that the POU covers the interval $[0, z_{\max}]$ and to minimize propagation errors do to velocity variations. The POU is used to window the wavefield into regions at each time step and the combination of windowing and Fourier transformation converts equation (3) into

$$U(\Delta t, x, z) = -U(-\Delta t, x, z) + 2\sum_{n=1}^{N} \mathbf{FT}^{-1}\left[ \cos\left( \omega_n(k_x, k_z)\Delta t \right) \mathbf{FT}\left[ \Omega_n(x,z) U(0,x,z) \right] \right], \qquad (4)$$

where $\omega_n\left(k_x,k_y\right)=v_n\sqrt{k_x^2+k_z^2}$, **FT** and $\mathbf{FT}^{-1}$ are forward and inverse 2D Fourier transforms, $v_n$ is the velocity used for propagation in the nth window, and we note that the windowed forward Fourier transform is essentially a Gabor transform.

## Examples

Equation (4) is used recursively to calculate the response to a minimum phase wavelet for a linear velocity medium $v(z)=1.5z+1000$. A partition of unity is displayed in Figure 2 with 9 windows. The impulse is a circle whose center of radius moves down in depth with time. The response to 5 minimum phase impulses in Figure 2 has good continuity and shows amplitude gradients along the wavefront as expected from geometric spreading.

A synthetic model of a salt dome is migrated by a poststack RTM. For comparison, the model is also migrated by finite differencing the wave equation. A synthetic model of the salt dome was generated using standard finite difference modeling. The high constant velocity salt dome is on the right side of the velocity model. While on the left, the velocity model has a constant gradient. Figure 3 is a comparison of the migrations. Both methods produced an acceptable image of the salt dome although the finite-difference method required finer spatial sampling and finer time stepping.

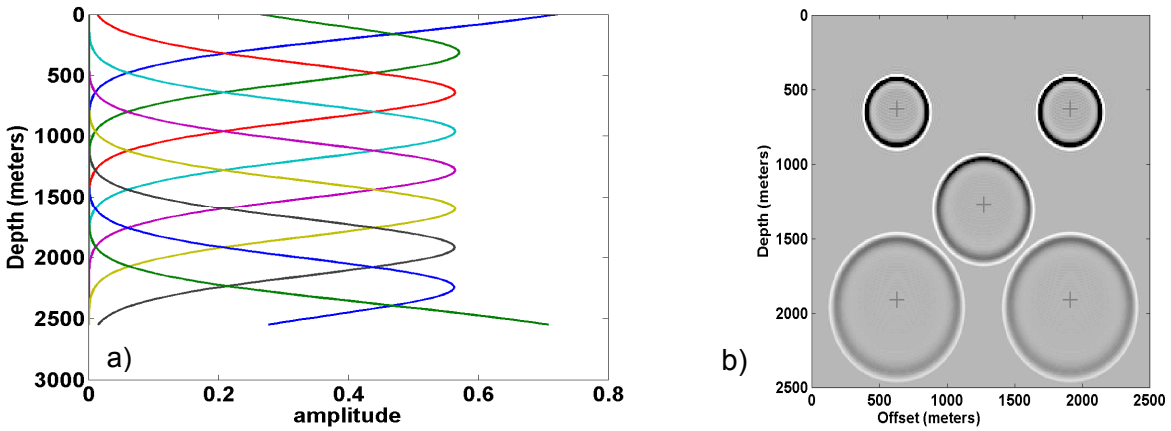


Figure 2: (a) A partition of unity with 9 windows. From 2560m to 3000 meters there is a zero pad to avoid wraparound effects from the Fourier transform. (b) The response to 5 minimum phase impulses in a medium with a constant velocity gradient.

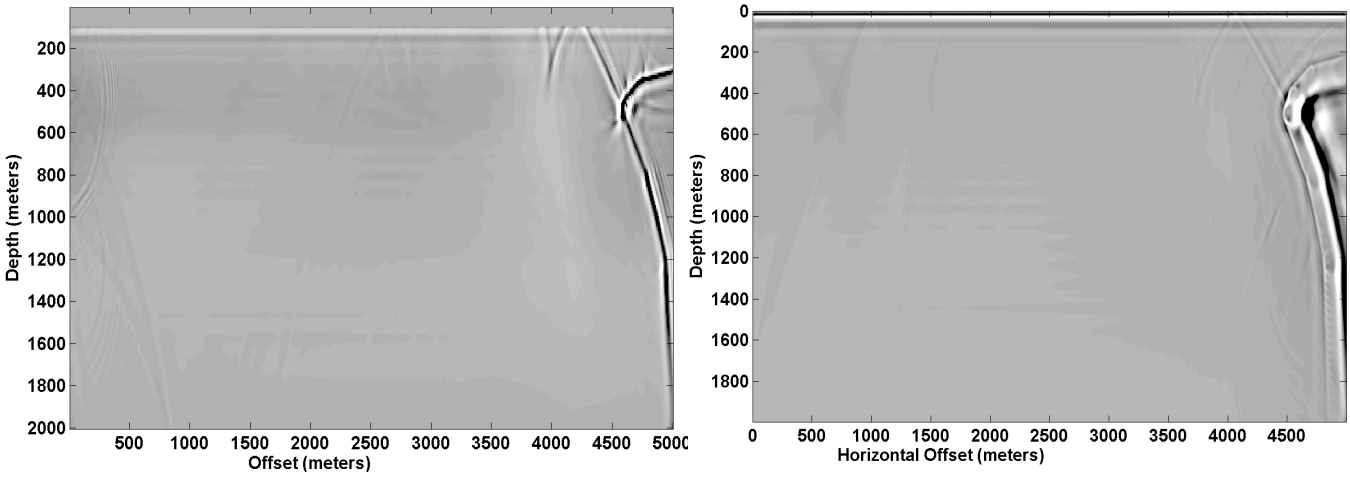


Figure 3: Left: A poststack migration of a saltdome model using equation (4). Right: A second-order finite-difference poststack RTM of a saltdome model.

## Conclusions

We proposed a Fourier domain time-stepping equation for RTM which is used to migrate a poststack image of a salt dome. Our method multiplies the spatial Fourier transform of the wavefield by a cosine whose argument depends on velocity and wavenumber. This can be interpreted as a spatial phase shift. For comparison, the salt dome was migrated by finite-difference time stepping the full wave equation. The two images were comparable in quality and the phase-shift time-stepping equation was computed in a fraction of the time.

## Acknowledgements

We thank the sponsors of the CREWES project, and those of the POTSI consortium, and especially NSERC, MITACS, PIMS, and Alberta Ingenuity.

### References

Baysal, E., Kosloff, D. D., and Sherwood, J. W. C., 1983, Reverse-time migration:, Geophysics, 48, 1514–1524.

Jones, I. F., Goodwin, M. C., Berranger, I. D., Zhou, H., and Farmer, P. A., 2007, Application of anisotropic 3D reverse time migration to complex North Sea imaging, SEG Expanded Abstracts **26**, 2140.

Ma, Y., and Margrave, G. F., 2007, Seismic depth migration using non-uniform Gabor frames: Ann. Internat. of the European Assoc. of Geoscientists and Engineers, Expanded abstracts.

McMechan, G. A., 1983, Migration by extrapolation of time-dependent boundary values, Geophysical Prospecting **31**, 413-420.

Whitmore, N. D., and Lines, L. R., 1986, Vertical seismic profiling depth migration of a salt dome flank, Geophysics **51,** 1087-1109.